Journal of the Korean Physical Society, Vol. 76, No. 10, May 2020, pp. 899∼903

Transition Between Severe and Mild Wear of 2024A-T4 Anodized Aluminum Alloy under Severe Wear Conditions

Nazih Tekkouk* and Mohamed Arbaoui
Université M'Hamed BOUGARA Boumerdes, FHC, Boumerdes 35000, Algeria

Saîd Abdi
Materials Science and Engineering Laboratory (LSGM), USTHB, Algiers 16123, Algeria

Amine Rezzoug
Research Center in Industrial Technologies (CRTI), P.O.Box 64, Cheraga, Algiers 16014, Algeria

(Received 28 January 2019; revised 10 February 2020; accepted 10 February 2020)

Aluminium alloys are gradually replacing grey cast iron in the automotive industry thanks to its low density. The purpose of this study is to evaluate tribological properties of 2024A anodized aluminium alloy under severe wear conditions. For this aim we are investigating the effect of the sliding speed and the anodic layer in order to improve the wear resistance and friction properties of 2024A aluminium alloy and this by using the latter with the hard metal chrome steel 100C6 in dry punctual contact. So we shall evaluate hardness, wear rate and friction properties after and before the anodizing process. The results have shown that the sliding speed affects a transition from severe wear to mild wear when $u = 0.3$ m/s for the alloy covered by hard anodic layer, as well as it was a significant decrease in wear rate.

PACS numbers: 61.05.−a, 64.60.−i, 68.05.Gh, 81.05.Bx, 68.08.−p
Keywords: Severe wear, Hard Anodizing, Sliding speed, Wear rate, Mild wear
DOI: 10.3938/jkps.76.899

I. INTRODUCTION

A great deal of research on wear characterization of grey iron has been conducted, for instance Terhech's [1] and Han's [2] works which were devoted to the study of the behavior of gray cast iron and its wear resistances under dry and lubricated conditions. Manufacturers are gradually replacing grey iron with aluminum alloys, which have good mechanical properties, because pure aluminum has poor mechanical properties. Researchers have conducted numerous studies with the objective of enhancing mechanical properties and the tribological performances of aluminum [3–11]. Figueroa's work [12] showed the wear behavior of cold-rolled and recrystallized AA1100 Al alloy and Al-Sn alloys, and he confirmed the essential contribution of Sn to the reduction of adhesive wear in Al-based alloys. Moreover, Pires [13] studied the influence of two coatings anodization and diamond-like carbon coating, on the wear resistance of the SAE 305 aluminum alloy. Anodization is an electrochemical process for producing an oxide coating (alumina) on the surface of a metal in order to increase its resistance to corrosion and abrasion [14,15]. This process can easily be realized without much cost. The electrolytic process is controlled by four factors [15]: the electrolyte concentration (Ce), the electrolyte temperature (T), the current density (di) and the processing duration (t). Conventional anodizing with sulfuric acid is done with the following parameter values: di = (1.2 – 1.5) A/dm^2 , Ce (H_2SO_4) = (180 – 220) g/l, T = (20 ± 5) °C, and t = (20 – 30) min. The thickness of the layer obtained by conventional anodizing is commonly on the order of ten micrometers [15], so we can increase the hardness of the oxide layer by changing the parameters that affect the anodizing process [15]: for instance at hard anodizing (HA), the affecting factor can be varied on: di = (2 – 3) A/dm^2, Ce (H_2SO_4) = (180 – 220) g/l, T = (5 ± 5) °C, and t = (40 – 60) min.

The 2024A aluminum alloy has good mechanical properties and is frequently used in aeronautic industry because of its excellent ability to adhere to the protective oxide layer of the substrate [16]. The anodic film is composed of a compact inner layer and a porous outer layer, which can be sealed to improve the corrosion resistance [16]. Bertrand [16] confirmed that anodized samples had better corrosion resistance due to the presence of an an-

*E-mail: n.tekkouk@univ-boumerdes.dz

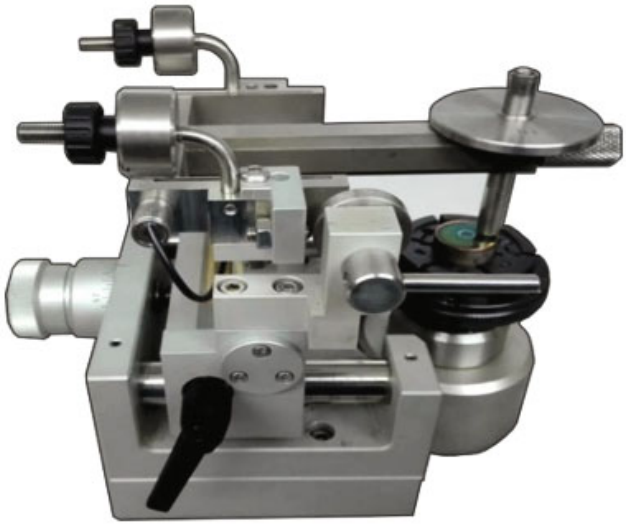

Fig. 1. CSM Pin-on-disk wear test machine.

odic film on the sample's surface. Thus, in our current study, we evaluated the properties of the anodic film on the surface of the 2024A, but in this case, we evaluated the friction and the wear properties of the alloy tested under severe wear with 100C6 chrome steel in dry conditions. Indeed, alloys that are not protected with an oxide layer exhibit a bad friction behavior under severe wear conditions. Moreover, we compare the mechanical characteristics of the alloy with those of grey cast iron. The coefficient of friction (COF) was chosen as the evaluation parameter for the tribological characteristics because it is a direct expression of the energy that is expended and dissipated as heat (E_d) according to Ref. 17, $E_d = Q \cdot u \cdot f$. A surface network of mechanical stresses evolves dangerously with increasing friction coefficient [17], which is why we tried to lower, as much as possible, the friction coefficient. For that purpose, we investigated the effect of the sliding speed on the wear resistance of the anodized alloy.

II. EXPERIMENTS AND DISCUSSION

The wear tests were performed using a pin-on-disk CSM Tribometer machine (Fig. 1). The pin of the test rig was a ball of chrome steel 100Cr6, and the samples were disks of 2024A alloys with dimensions of $30 \times 35 \times 8$ mm^3. A steel ball slides on the flat face of a sample while rotating in the horizontal plane. The load and the speed were controlled for measuring the friction. The samples were prepared on a contact surface before each test by using abrasive paper up to 1200 μm roughness, and a Taylor Hobson stylus profilometer was used to measure the arithmetic mean roughness (Ra) for each sample.

The chemical composition of the metals was determined using energy dispersive X-ray fluorescence spectrometer, and the results are presented in Table 1.

Table 1. Chemical composition of 2024A-T4.

Chemical composition (%)						
Al	Cu	Mg	Si	Fe	Mn	Zn
Rest	3.99 – 4.009	1.699 – 1.753	0.331	0.329	0.238	0.078

Table 2. Hardness measure.

Spécimen	2024A
Hardness Range (HV)	135

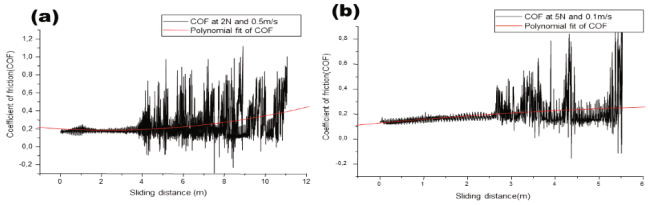

Fig. 2. COF (f) under dry conditions for (a) Q = 2 N, u = 0.5 m/s and (b) Q = 5 N, u = 0.1 m/s.

The hardness measure of the alloy as the disk is indicated in Table 2, the condition tests are represented in Table 3 and the results of tests are shown in Fig. 2.

Figures 2(a) and 2(b) illustrate that the values of COF (f) are never stable. In Fig. 2(a) even so the load is low (Q = 2 N) but the COF is high (f = 0.8) after a 4m sliding distance and after a 11m sliding distance, the COF is 1. In Fig. 2(b) the load charge is increased (Q = 5 N) and the velocity is decreased (u = 0.1 m/s) but always the COF value is high, f = 1 after a 5m sliding distance, we note that the sliding distance in the second case is shorter than the first because the load is increased. We notice that the tribometer is programmed to stop at f = 1 to avoid vibrations due to seizure. Thus, a bad friction behavior is present in both cases because the values of COF are always high in both tests. Thus we can consider that the 2024A aluminum alloy under those conditions is showing severe wear.

Anodizing was carried out in the laboratory with sulphuric acid at Ce = (200 g/l H_2SO_4) and T = (5 ± 5) °C. The initial temperature was T_0 = 0 °C. Lead was used as the cathode and the aluminum alloy was used as the anode, di = 3 A/dm^2, and t = 60 min. After anodizing, specimens wash in distilled water and after that are sealed with drilling distilled water for t = 60 min in the objective to close the pores formed in the outer layer for the oxide coating (Fig. 3).

The hardnesses of the samples were measured at different roughnesses before and after the anodizing processes by using the Vickers test at 0.5 kgf and the results are given in Table 4.

In Table 4, we note that there is a significant ameliora-

Table 3. Tests conditions.

Conditions	Sample	Ra (µm)	Load (N)	Sliding speed (m/s)	Sliding distance (m)
Dry	5	0.22	2	0.5	100
	6	0.22	5	0.1	100

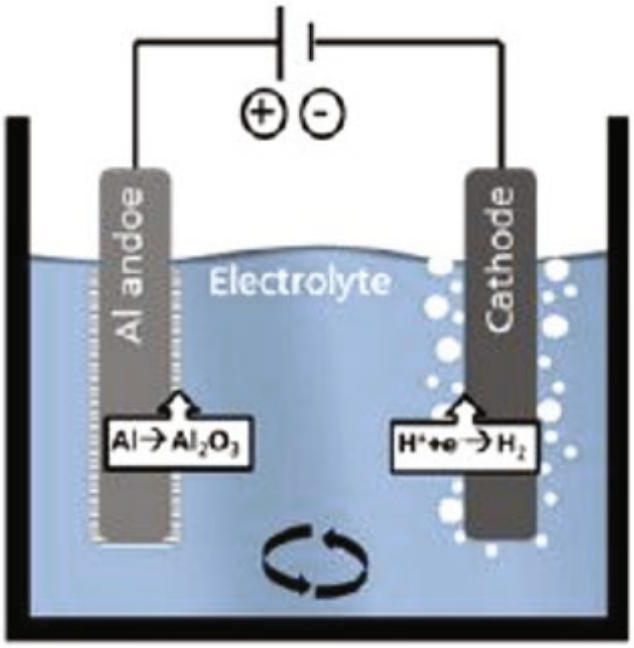

Fig. 3. Anodizing process.

Table 4. Hardness results.

Al-Cu-Mg alloy samples	Ra (µm)	Micro Hardness
Before anodizing	0.22	H = 135 HV
After anodizing	0.26	305 HV
grey cast iron (SAE G-3500) [1]	/	207 – 255 HV

tion of almost 26% in the hardness after anodizing, and the hardness value is greater than for that of grey cast iron [1]. Next we evaluated the friction and the wear performance of the anodized alloy. Figure 4 show scanning electron microscopy (SEM) images of the oxide layer obtained by hard anodizing; the thickness of the oxide layer is seen to be about 40 µm (Fig. 4(b)). In that figure, the wall of the oxide cells in the outer anodic layer contains a few particles, wheel are due to the dissolution of element of copper (Cu) in the anodic layer [18].

Figure 5 presents the X-ray diffraction (XRD) pattern of the anodic alloy, we note that the indexation of the diffraction peaks was made by using the ASTM sheet [18,19]. Seven apparent peaks of alumina (αAl_2O_3) with different intensities can be seen in Fig. 5.

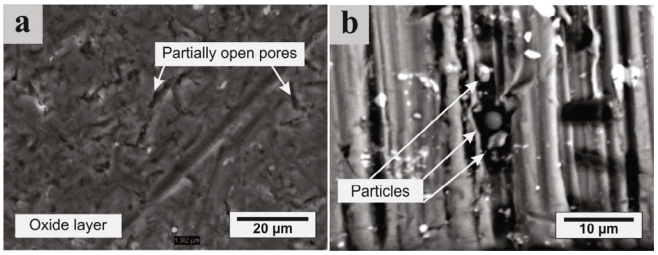

Fig. 4. SEM image of the anodic layer. (a) Morphology of the surface of the coating and (b) Side view of the anodic layer.

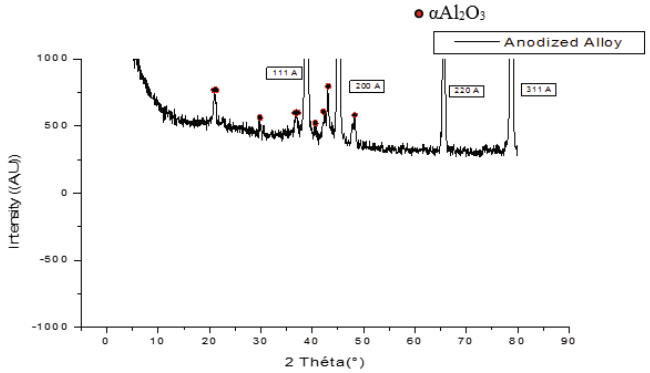

Fig. 5. XRD results of the alloy covered by hard anodic layer.

After anodizing we investigate the effect of sliding speed, the operating conditions are mentioned in Table 5. The wear volume (V) is measured by using the equation $V = \frac{P \cdot \left(\frac{L}{2}\right) \cdot 2\pi \cdot r}{2}$ [20]. Where P is the Depth of trace (µm) and L is the Width of the trace (µm).

The wear rate is calculated by using the equation $k = V/L$ [21]. The values of k are reported in the Table 5.

Figure 6 shows the profiles of the wear tracks, thus the profiles were traced by using HOMMEL-ETAMIC profilemeter. The profile 1 in Fig. 6(a) presents the wear track when $u = 0.5$ m/s, and the profile 2 corresponds to the wear test when $u = 0.3$ m/s. The depth and the width of the profile 2 in Fig. 6(a) are smaller than of the all of the widths and the depths of profiles presented in Fig. 6. The profile at $u = 0.3$ m/s measured the smallest wear volume loss, in this speed we considered the anodised alloy gives the best wear resistance, and the results of the wear volumes of all the tests are modelled in Fig. 7.

Table 5. Tests conditions.

n°	H (MPa)	Ra (µm)	Q (N)	u (m/s)	t (mn)	L (m)	V (mm^3)	K (10^{-2} mm^3/m)	f
8	305	0.26	10	0.2	16	200	1.06	0.5	0.443
9	305	0.26	10	0.3	16	288	0.09	0.03	0.384
10	305	0.26	10	0.4	16	384	0.8	0.2	0.421
11	305	0.26	10	0.5	16	500	0.6	0.1	0.390

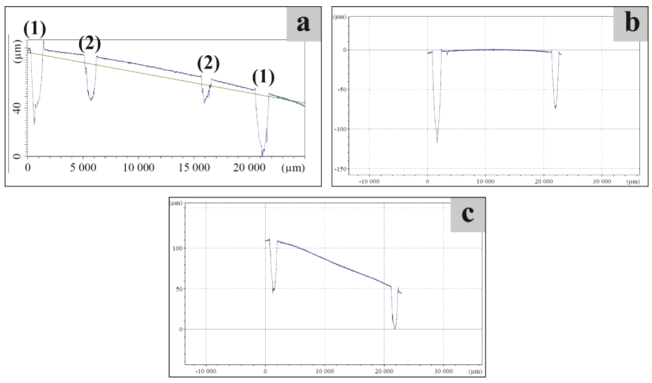

Fig. 6. Profile of the wear tracks at different speeds: (a) (1) u = 0.5 m/s, (2) u = 0.3 m/s, (b) u = 0.2 m/s and (c) u = 0.4 m/s.

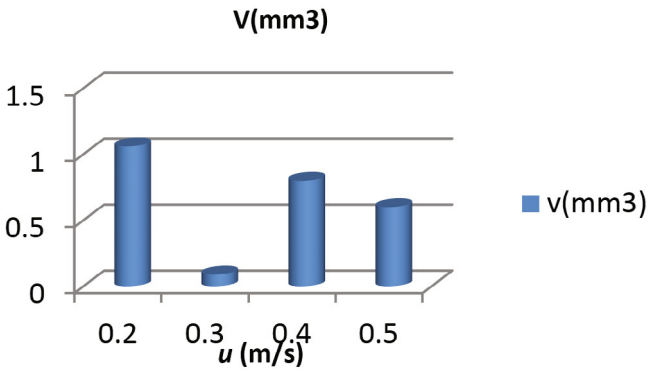

Fig. 7. Wear volume at different sliding speed.

We note viewing the results of Table 5 that there is an improvement in COF (f) and in wear rate (K) when u = 0.5 m/s and u = 0.3 m/s as well as the wear volume compared with the other values, we can be conclued that the equation $E_d = Q \cdot u \cdot f$ isn't always validate because when u = 0.3 m/s the value of COF is smaller than when u = 0.2 m/s, and when u = 0.5 m/s the value of COF is smaller than when u = 0.4 m/s.

Likewise, it is interesting to note that the minimum wear rate (K = $0.03 \cdot 10^{-2}$ mm^3/m) is reached at the sliding speed, 0.3 m/s, according to Ref. 21 the wear regime of the alloy is founded in mild wear regime because ($10^{-4} < K \leq 10^{-3}$), on the other hand the others

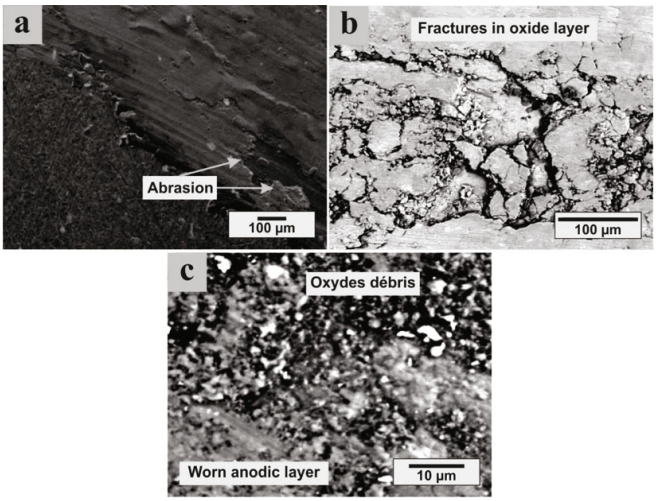

Fig. 8. Wear tracks of HA: (a) track morphology and (b, c) abrasive wear track.

values of wear rate are founded in the severe wear regime because ($10^{-3} < K \leq 10^{-2}$) [21]. According to Ref. 21 there is a transition from severe to mild wear when u = 0.3 m/s. We can explain this transition when the speed increase, the temperature at the contact influences the structure in the layers of alloy which lead to the increase of their hardness and certain mechanical characteristics [22], which is the reason to reduce their volume loss of wear, so we can considered the speed at u = 0.3 m/s is the threshold value [23].

The Fig. 8 shows the different consequences of wear resulting from the degrees of shock exerted by the peers, we start with increasing order of degrees of deformation, and we have the following.

Adhesion

✓ *Swollen layer*: In Fig. 8(a), the anodic layer is swollen and appears to be dissolved due to the effect of heat dissipated by friction and it contains grooves.

✓ *Grooves*: In Fig. 8(a), the features on less deep.

Abrasion

✓ *Cracks*: At the beginning of plastic deformation, small holes that are wider and deeper than the grooves are clearly visible (Fig. 8(a)).

✓ *Fracture*: The crack begins to widen and enlarge

because of the cumulative shocks exerted by the peers, and a crack propagates and become several cracks are seen in Fig. 8(b).

✓ *Tearing of layer*: Due to the cyclic stresses exerted by the pairs, the thickness of the oxide layer will decrease, and the fractures will disappear and become scattered oxide debris everywhere on the surface of the alloy (Fig. 8(c)).

✓ *Perforation*: In the end, the oxide layer is totally deteriorated, and the substrate is clearly visible as it is unmasked as seen in Fig. 8(a).

Table 6. Nomenclatures.

Parameters	Definition
d	Density (kg/dm^3)
E	Young's module (GPa)
E_d	Energy dissipated (J)
f	Dynamic friction coefficient
H	Hardness (MPa)
L	Sliding distance (m)
Q	Normal load (N)
Ra	Arithmetic mean roughness (μm)
u	Sliding velocity (m/s)
Abbreviations	**Definition**
COF	Coefficient of friction
HA	Hard anodizing
Ce	Concentration (g/l)
di	Current density (A/dm^2)

III. CONCLUSION

The hard anodizing process increases the hardness of the 2024A aluminum alloy, which enhances the wear properties of the alloy under severe wear conditions. Increasing sliding speed affects dissipation of the structures due to a kinetic phase transition that occurs under the synergistic actions of strain, mass transfer and heating, which increases the hardness and there by affects the transition from severe wear to mild wear for the anodized alloy. The friction coefficient is a direct expression of the wear rate of the alloy, but the wear rate does not depend on the COF value. Mechanical properties of the optimum speed are guaranteed by the anodic layer due to its large homogenous oxide thickness. Also, an anodic layer with greater hardness guarantees the best wear resistance.

ACKNOWLEDGMENTS

We would like to express our deepest appreciation to all those who provided us with possibility to complete this work. Special gratitude is given to the Supmeca the Higher Institute of Mechanics of Paris, whose contribution to the characterization of the experimental trials was essential. We also thank the AMC research direction in Tipasa for their hospitality and patience in receive us in its chemistry laboratory.

REFERENCES

[1] M. Terheci, R. R. Manory and J. H. Herde, Wear **180**, 73 (1995).
[2] J. M. Hana *et al.*, Wear **271**, 1854 (2011).
[3] D. Huang, W. Chen, S. Zhang and Z. He, Trans. Nonferrous Met. Soc. China **20**, 54 (2010).
[4] S. Temel and B. Osman, Tribol. Int. **43**, 1346 (2010).
[5] S. Temel and Y. Alemdag, Mater. Sci. Eng. A **496**, 517 (2008).
[6] M. M. H. Bastwros, A. M. K. Esawi and A. Wifi, Wear **307**, 164 (2013).
[7] M. Parikshit, R. K. Dube, B. Bikramjit and S. C. Koria, Surf. Coat. Technol. **203**, 3541 (2009).
[8] A. Devaraju, A. Kumar, A. Kumaraswamy and B. Kotiveerachari, Mater. Des. **51**, 331 (2013).
[9] G. Vivek, R. Sellamuthu and A. Sanjivi, Procedia Eng. **97**, 1355 (2014).
[10] F. Chen *et al.*, Trans. Nonferrous Met. Soc. China **25**, 103 (2015).
[11] A. Kumar, M. Mahapatra and P. K. Jha, Wear **306**, 170 (2013).
[12] C. G. Figueroa, V. H. Jacobo, A. Ortiz and R. Schouwenaars, Tribol. Lett. **59**, 27 (2015).
[13] M. S. T. Pires *et al.*, Tribol. Lett. **66**, 52 (2018).
[14] M. Whelan, J. Cassidy and B. Duffy, Surf. Coat. Technol. **235**, 86 (2013).
[15] F. Gilbert, Thèse de doctorat. Université Laval Québec, 2011.
[16] B. Priet *et al.*, Surf. Coat. Technol. **307**, 206 (2016).
[17] M. Cartier and P. Kapsa, Technique de l'ingénieur, BM 5065-6 (2012).
[18] C. Fares *et al.*, Mater. Des. **86**, 723 (2015).
[19] JCPDS ICDD carte N°04, 0787 (1997).
[20] J. Escobar, Doctorat de l'université de Toulouse. (2013), Chap. IV, p. 145 .
[21] J. Zhang and A. T. Alpas, Acta Mater. **45**, 513 (1997).
[22] B.I. Kostetsky, Wear **159**, 1 (1992).
[23] M. Ruiz-Andrés, A. Conde, J. de Damborenea and I. García, Tribol. Trans. **58**, 955 (2015).